

# Instability and front propagation in laser-tweezed lipid bilayer tubules

Peter D. Olmsted\* and F. C. MacKintosh

Department of Physics, University of Michigan, Ann Arbor MI 48109-2210  
(October 29, 2018)

We study the mechanism of the ‘pearling’ instability seen recently in experiments on lipid tubules under a local applied laser intensity. We argue that the correct boundary conditions are fixed chemical potentials, or surface tensions  $\Sigma$ , at the laser spot and the reservoir in contact with the tubule. We support this with a microscopic picture which includes the intensity profile of the laser beam, and show how this leads to a steady-state flow of lipid along the surface and gradients in the local lipid concentration and surface tension (or chemical potential). This leads to a natural explanation for front propagation and makes several predictions based on the tubule length. While most of the qualitative conclusions of previous studies remain the same, the ‘ramped’ control parameter (surface tension) implies several new qualitative results. We also explore some of the consequences of front propagation into a noisy (due to pre-existing thermal fluctuations) unstable medium.

PACS: 47.20.Dr, 47.20.-k, 47.20.Hw, 82.65.Dp

Short Title: **Dynamic instability in bilayer tubules.**

## 1. INTRODUCTION

A recent series of exciting experiments [1] demonstrated a dynamic instability induced on tubules of single lipid bilayers by application of laser ‘tweezers’, whereby the cylindrical tubule of radius  $R_0$  modulates with a wavenumber given by  $q^*R_0 \simeq 0.8$ . This instability has been attributed to an excess surface tension due to the gain in electrostatic energy when surfactant molecules, of higher dielectric constant than water, displace water in the electric field of the laser.

The starting point for understanding this phenomenon is the Rayleigh instability [2–4] of a thin cylindrical thread of liquid with positive surface tension, whereby the thread can reduce its surface area at fixed volume by modulating and evolving towards a string of beads. Rayleigh calculated the preferred wavelength of a cylinder of fluid in air in the inviscid [2] and non-inertial (viscous) [3] limits, finding in the former case a characteristic non-zero wavenumber and in the latter case a preferred wavenumber of zero (or infinite wavelength). Later, Tomotika [4] calculated the instability for a viscous fluid surrounded by another viscous fluid, again in the non-inertial regime, finding that the change in boundary conditions restores a finite characteristic wavelength. See Olami and Granek [5] for a discussion of this point. The present problem, however, requires a much different detailed dynamical analysis which relates the flow of lipid molecules in the interface to the bulk flow in the surrounding fluid. An important physical ingredient is a new conserved quantity, the lipid on the surface.

At present there are (at least) two theoretical treat-

ments of the experiments of Ref. [1]. Bar-Ziv and Moses [1] and Nelson and co-workers [6] have proposed the picture that the surface tension rapidly equilibrates everywhere to an induced value  $\Sigma_0$ , and the instability proceeds from this state. In contrast, Granek and Olami [5] have postulated that the correct treatment of the problem is to impose a constant rate at which lipid molecules are drawn into the trap from the tubule. This loss of lipid is accommodated by stretching out small wavelength surface fluctuations and the result is again a uniform surface tension  $\Sigma_0$ . Goldstein, *et al.* (GNPS) [7] demonstrated quantitatively how the equilibration of the tension in the tube stays ‘ahead’ of a shape change, so that a treatment with a constant (in time) surface tension is reasonable; and argued that the primary loss of area is in the shape instability itself, rather than through the removal of small-scale wrinkles.

We propose a slightly different picture of the steady state before the onset of the instability, which follows from consideration of the experimental configuration. The tubules, as formed, are several hundred microns long and are attached at either end to ‘massive lipid globules’ [1] of order  $10\mu\text{m}$  in diameter. Hence, the tubules must be in contact with a reservoir which fixes the lipid chemical potential (or, equivalently, the surface tension). If we assume the system is equilibrated, it follows that the chemical potential for exchange between the tubule, reservoir, and solvent/lipid bath vanishes [8], and we may assume a reference chemical potential of zero or, equivalently, zero surface tension. This coincides with the experimental observation of visible thermal fluctuations on the tubules [1].

---

\*e-mail: [phy6pdo@irc.leeds.ac.uk](mailto:phy6pdo@irc.leeds.ac.uk); permanent address, Dept. of Physics, University of Leeds, Leeds LS2 9JT, UK

Now imagine applying a laser to the tubule. In the electric field of the chemical potential of a lipid molecule is lowered by an amount  $\delta\epsilon\mathcal{E}Da$ , where  $D$  is the molecular length,  $\delta\epsilon$  is the dielectric constant relative to water,  $a$  the area of the lipid, and  $\mathcal{E}$  the energy density deposited in the trap. Nelson *et al.* [7] calculated that this yields an energy gain per area of bilayer of  $\Sigma_0 \sim 2 \cdot 10^{-3}$  erg cm<sup>-2</sup>, for a laser power of 50 mW.

Hence there is a large reduction in the local chemical potential as the lipid suddenly finds it advantageous to move into the laser spot. The surface tension in the adjacent portion of the tubule increases as lipids start to move out of the surface. Since the other end of the tubule is in contact with a reservoir at zero chemical potential, the final state (prohibiting, for the moment, surface undulations) must be a non-equilibrium steady state in which:

1. Lipid is transported at constant velocity from the reservoir at zero chemical potential to the laser trap at a negative chemical potential.
2. The chemical potential drops linearly along the tubule, with a gradient that balances the frictional drag of the bulk fluid in steady state.
3. The local lipid concentration also varies linearly, since the two-dimensional lipid fluid membrane is compressible.

This differs significantly from the treatments of Nelson *et al.* and Granek and Olami in that *lipid must flow out of the anchoring globules* and the chemical potential (or surface tension) never attains a non-zero constant over the duration of the experiment. In fact, prohibiting the shape instability, the boundary conditions specified by both Olami and Granek and Nelson *et al.* yield a tense final state as (a small amount of) area is drawn out of surface fluctuations, while the treatment of the anchoring globules as reservoirs yields the steady-state described below.<sup>(1)</sup>

Several consequences follow from this observation. First, a chemical potential gradient suggests a mechanism for front propagation [7,9]. The front starts at the laser spot where the surface tension is largest, and ‘propagates’ outward toward the anchoring globule simply because the amplitude of the instability grows at different rates along the tube. Our results predict a speed of front propagation which is inversely proportional to the length of the tube, and is largest near the laser spot, decreasing to zero somewhere near the anchoring reservoirs; and a characteristic wavenumber which also decreases (much slower, see Fig. 5 below) away from the laser spot.

---

<sup>(1)</sup>If we wait long enough the trap will ‘fill up’ with surfactant and the chemical potential return to zero everywhere. However, in the present case of strong laser power the surface instability will have occurred by this time. See Section 3.3.

The outline of this paper is as follows. In Section 2 we derive the linear concentration gradient in the absence of surface undulations. We predict a ‘ramped’, or spatially-varying control parameter, the effective surface tension, which is in fact the two-dimensional pressure whose gradient drives the flow of lipid against the viscous drag of the bulk fluid. In Section 3 we present a detailed microscopic picture of the uptake of surfactant by the trap, and argue that a competition between bending and compression energies modifies the effective surface tension of the trap. This leads to a prediction of a critical laser power for the onset of an instability. While this section may safely be omitted in reading this paper, it illuminates the nature of the instability by treating a realistic scenario for how the trap buckles to initiate flow.

In Section 4 we discuss the implications of a slowly varying surface tension on the detailed calculation of Goldstein, *et al.* [6,7]. We also discuss front propagation within the picture of a surface tension gradient, which relates the problem to a large body of work on front propagation with ‘ramped’ parameters [10]. The issue of front propagation in this system is delicate [7], and our results suggest at least two possibilities, which we briefly raise in this work and pose for further investigation. Depending on whether noise (*i.e.* existing thermal fluctuations in the tubule) is present, we expect front propagation which is either (a) characteristic of that predicted by the so-called Marginal Stability Criteria (MSC) [7,10], or (b) dominated by amplification of existing ‘noise’, which can lead to behavior reminiscent of front propagation for a steep enough ramp. We conclude in Section 5 by recalling the relevant timescales and frequencies, and summarizing our predictions and the differences from previous treatments.

## 2. STEADY STATE

In this section we calculate the steady-state configuration of a tubule under the action of an applied laser intensity, assuming the laser supplies a chemical potential  $-\Sigma_0$  at the laser spot. Note that this implies a reservoir in which to pack lipid molecules. In Section 3 we support this with a microscopic picture which leads to virtually the same results that we obtain in this section, with a prefactor of order one which depends on the laser shape. Note that there are several possible microscopic scenarios for initiating flow into the trap, and Section 3 addresses only one of these.

## 2.1. Equations of motion

Changes in chemical potential  $\delta\mu$  are related to changes in surface tension  $\delta\Sigma$  by  $\delta\mu = -\phi^{-1}\delta\Sigma$ , where  $\phi$  is the lipid concentration (and hence  $\phi^{-1} = a$  is the area per lipid). Also,

$$\Sigma = -p, \quad (2.1)$$

where  $p$  is the 2-dimensional pressure of the fluid of lipid molecules.

The geometry of the system is taken as shown in Figure 1, with the cylinder aligned parallel to the  $z$ -axis and  $r$  the radial coordinate. The boundary conditions are

$$p(z=0) = 0 \quad (\text{reservoir}) \quad (2.2)$$

$$p(z=L) = -\Sigma_0 \quad (\text{laser spot}), \quad (2.3)$$

where  $\Sigma_0$  is the surface tension induced by the laser.

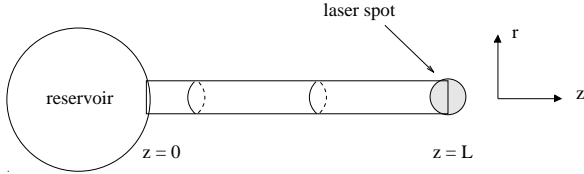


FIG. 1. Geometry of lipid tubule under localized tension.

The Navier-Stokes and continuity equations for the 2D fluid of lipid molecules are

$$\partial_t \phi = -\nabla \cdot (\phi \mathbf{v}) \quad (2.4)$$

$$\rho_s (\partial_t + \mathbf{v} \cdot \nabla) \mathbf{v} = \eta_s \nabla^2 \mathbf{v} + \left(\frac{1}{3}\eta_s + \gamma_s\right) \nabla (\nabla \cdot \mathbf{v}) - \nabla p + \Delta \mathbf{T}^b \cdot \hat{\mathbf{r}}. \quad (2.5)$$

Here  $\eta_s$  and  $\gamma_s$  are 2D shear and bulk viscosities,  $\rho_s$  is 2D lipid mass density, and  $\Delta \mathbf{T}^b \cdot \hat{\mathbf{r}}$  is the viscous drag acting on the surface from the dissipative stress tensor  $T_{\alpha\beta}^b = \frac{1}{2}\eta(\nabla_\alpha u_\beta + \nabla_\beta u_\alpha)$  in the surrounding fluid. This flow is established in a vorticity diffusion time  $\tau_v$  which is much smaller than other times in the problem. We ignore drag from outside the cylinder for the moment, since this flow essentially moves with the surfactant molecules and contributes relatively little to the boundary stress<sup>(2)</sup>.

With the above approximation, the boundary stress is given by the shear stress in the tube. For a *uniform* flow of lipid  $\mathbf{v} = v\hat{\mathbf{z}}$ , the interior flow is Poiseuille [11],

$$\mathbf{u}(r) = v \frac{2r^2 - R_0^2}{R_0^2} \hat{\mathbf{z}}, \quad (2.6)$$

where  $R_0$  is the tube radius and we use the no-slip boundary condition  $u(r=R_0) = v$ . Hence the stress acting on the surface is

$$\Delta \mathbf{T}^b \cdot \hat{\mathbf{r}} = -\frac{2\eta v}{R_0}. \quad (2.7)$$

Gradients of  $\mathbf{v}$  in the  $z$ -direction change the flow profile from simple Poiseuille, but this has only a very small effect on the dynamics of establishing the steady state, primarily in the region of the laser spot, which we ignore for now.

The final ingredient we need is the compressibility of the film, through the constitutive relation

$$p = p_0 - \chi^{-1} \delta a \quad (2.8)$$

where  $p_0$  is the equilibrium pressure.

Now we specialize to the problem at hand. We linearize the dynamic equations in  $\mathbf{v}$  and  $\delta\phi = \phi - \phi_0$ , assume a velocity of the form  $\mathbf{v} = v(z)\hat{\mathbf{z}}$ , and ignore the inertial term in the Navier-Stokes equation. Employing Eq. (2.8), we obtain

$$\partial_t \delta\phi = -\phi_0 \nabla_z v \quad (2.9)$$

$$0 = \hat{\eta} \nabla_z^2 v - B \phi_0^{-1} \nabla_z \delta\phi + \frac{2\eta}{R_0} v, \quad (2.10)$$

where  $\hat{\eta} = \frac{4}{3}\eta_s + \gamma_s$ .

The boundary conditions are

$$\delta\phi(z=0) = 0 \quad (2.11)$$

$$\delta\phi(z=L) = \phi_0 \Sigma_0 / B. \quad (2.12)$$

where  $B = \chi^{-1} \phi_0^{-1}$  is the two dimensional bulk modulus.

## 2.2. Dynamics of equilibration

Assigning  $\delta\phi(z, t) = \delta\hat{\phi}(q, \omega) e^{i(qz - \omega t)}$  and similarly for  $v(z, t)$ , we obtain the following dispersion relation:

$$\omega = \frac{iBq^2}{q^2 \hat{\eta} + 2\eta/R_0}. \quad (2.13)$$

This yields  $\omega \simeq iR_0 B q^2 / \eta$  for  $q \ll q^*$  and  $\omega \simeq B / \hat{\eta}$  for  $q \gg q^*$ , where  $q^* = \sqrt{2\eta / (R_0 \hat{\eta})}$ . Hence, at long wavelengths we have diffusive behavior governed by the friction against the bulk fluid, while at short wavelengths the dynamics is dominated by the 2D viscosity. The crossover length is given by  $1/q^* \sim 0.1\mu\text{m}$ , where we have taken  $\eta \sim 10^{-2} \text{ g cm}^{-1} \text{ s}^{-1}$ ,  $\hat{\eta} \sim 10^{-6} \text{ g s}^{-1}$ , and  $R_0 \sim 0.5\mu\text{m}$ . Hence in most cases of interest we are in the regime dominated by bulk fluid dissipation and may ignore  $\hat{\eta}$ .

<sup>(2)</sup>We may include this as, for example, the Stokes drag on a cylinder, which increases the right hand side of Equation 2.7 by of order 10% [11].

We can now estimate (within linear response) the time to attain steady state after imposing the localized tension by the laser as, roughly, the relaxation time of the slowest mode given by the dispersion relation Eq. (2.13). Taking  $q = 2\pi/L$ , we have

$$\tau_{ss} \sim \frac{2L^2\eta}{(2\pi)^2 R_0 B} \sim 10^{-5} \text{ s}, \quad (2.14)$$

for  $B \sim 150 \text{ erg cm}^{-2}$  [12] and  $L \sim 100 \mu\text{m}$ . This estimate of  $B$  is a zero-temperature estimate and ignores small-scale thermal fluctuations which soften this modulus considerably [13,7]. As we discuss in the conclusion and as shown in Reference [7], this effect can reduce  $B$  by up to three orders of magnitude, increasing  $\tau_{ss}$  accordingly, to of order  $10^{-2} \text{ s}$ . We can compare this to the vorticity diffusion time,

$$\tau_v = \frac{\rho R_0^2}{\eta} \sim 10^{-7} \text{ s}, \quad (2.15)$$

where we take  $\rho = 1 \text{ g cm}^{-3}$ . Since  $\tau_{ss} > \tau_v$  our assumption above of a uniform shear stress is reasonable.

### 2.3. Steady State

To find the steady state we equate the left hand side of Eq. (2.9) to zero, which yields a constant velocity  $\bar{v}$ . From Eq (2.10)  $\nabla_z \delta\phi$  is also a constant and, applying the boundary conditions and the pressure constitutive equation, Eq. (2.8), we find the following steady-state profile

$$\bar{v} = \frac{R_0 \Sigma_0}{2\eta L} \quad (2.16)$$

$$\delta\phi = -\phi_0 \frac{\Sigma_0}{B} \frac{z}{L} \quad (2.17)$$

$$\delta\Sigma = \Sigma_0 \frac{z}{L}. \quad (2.18)$$

Thus we find that the steady state, excluding modulations of the cylinder, is a non-equilibrium steady state, where the lipid molecules run down a chemical potential gradient and the molecular spacing increases to reflect this changing local potential. An estimate above yields  $\bar{v} \sim 1 \mu\text{m s}^{-1}$ , where we use  $\Sigma_0 \sim 10^{-3} \text{ erg cm}^{-2}$ . The effective surface tension (or two dimensional pressure) is induced by the applied laser, and is non-zero *only in the presence of flow*.

## 3. MICROSCOPIC PICTURE

We have shown how lipid flow, which is a necessary condition for an effective non-zero surface tension far from the trap, follows from a boundary condition of fixed chemical potential at the trap. In this section we argue that this boundary condition requires an instability in

the trap, and we present detailed calculations for a possible scenario for the trap to initiate flow. We stress that there are several possible mechanisms, including buckling, ejection of micelles or bilayer structures, and growth of ‘cancerous’ membranes. This is surely not an exhaustive list.

### 3.1. Basic Considerations

We first note that a laser spot centered at  $z = L$  typically has a Gaussian intensity profile [14], which leads to an energy gain per area of lipid  $\mathcal{U}(z) = -\Sigma_0 \zeta(z)$ , with

$$\zeta(z) = e^{-(z-L)^2/2\Delta^2}. \quad (3.1)$$

The spot radius was estimated to be  $\Delta \simeq 0.15 \mu\text{m}$  in the experiments of Bar-Ziv and Moses [1].

We can envision two scenarios after applying the laser:

- (a) Lipid can be sucked into the trap until the electrostatic energy gain balances the cost of compressing the molecules in the bilayer. At this point the trap is full, flow stops, and the chemical potential (and surface tension) of the entire tube reverts back to zero.
- (b) For a critical tension  $\Sigma^*$  (Eq. 3.16) we expect the compressed section of the tubule to become unstable with respect to buckling. For higher intensities the trap continues to fold to accommodate more lipid, initiating a flow along the tubule. This flow must be accompanied by a chemical potential (or surface tension) gradient, which drives the instability seen in the experiments.

Our discussion suggests that the trap boundary condition should contain the physics that, at a certain distance from the center of the trap, lipid is incorporated into folds to relieve the in-layer compression. A reasonable choice is

$$a(z = L - \bar{\Delta}) = a_0, \quad (3.2)$$

where  $\bar{\Delta}$  is a distance to be determined. This asserts that the area per head assumes its preferred equilibrium value at the point where the folding begins.

In the next two subsections we derive the steady-state flow into the trap (prohibiting for the moment the ‘pearling’ shape change). We first obtain a general relation for the local area per lipid  $a(z)$ , which depends on the trap boundary condition. We then deduce a crude criterion for the position  $z = L - \bar{\Delta}$  at which the trap buckles. Applying the *assumption* of Eq. (3.2) at this position then yields the desired profile and steady-state flow.

### 3.2. Detailed Steady State

Let us examine the steady state. The continuity equation, Eq. (2.4), yields the condition

$$v(z) = Ca(z), \quad (3.3)$$

where  $C$  is a constant to be determined. Hence the steady-state Navier-Stokes equation, ignoring the 2D viscosity, becomes

$$0 = \frac{2\eta Ca(z)}{R} + \chi^{-1} \nabla_z a(z) - \nabla U(z). \quad (3.4)$$

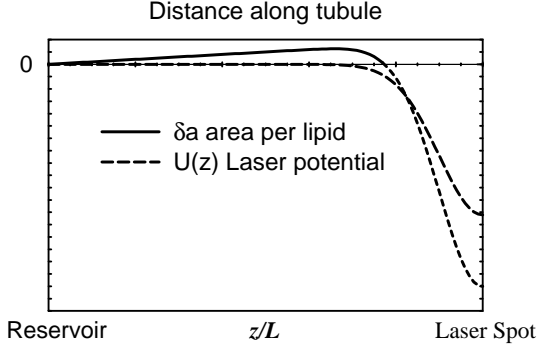


FIG. 2. Profiles for steady-state deviation  $\delta a$  in the area per lipid and the potential set up by the laser after buckling has occurred. The dotted line shows the continuation of  $\delta a$  (Eq. 3.5) into the buckled trap region beyond the point  $z = L - \bar{\Delta}$ , and should actually be replaced with buckled membrane at  $\delta a = 0$ . The boundary conditions are: (1)  $\delta a = 0$  at the reservoir, due to fixed chemical potential; and (2)  $\delta a(z = L - \bar{\Delta}) = 0$  (see Eq. 3.2). In steady state  $\delta a$  increases linearly away from the reservoir because the membrane is under tension, which varies linearly to counteract the viscous drag due to lipid flow.

The solution of this equation with the boundary condition  $a(0) = a_0$ , which follows from contact with a reservoir at ambient pressure, is

$$\frac{\delta a}{a_0} = e^{\lambda z} - 1 - \gamma \int_0^z ds e^{-\lambda(s-z)} \frac{\partial}{\partial s} \zeta(s) \quad (3.5)$$

$$\lambda = \frac{2\eta\chi C}{R_0}, \quad (3.6)$$

$$\gamma = \frac{\Sigma_0}{B}, \quad (3.7)$$

where  $\lambda$  is determined by the boundary condition at the trap. Note that  $\gamma \sim 10^{-5}$ , since  $\Sigma_0 \sim 10^{-3} \text{ erg cm}^{-2}$  and  $B \sim 150 \text{ erg cm}^{-2}$ . Using Eq. (3.2), we find

$$\lambda = \frac{-\gamma \zeta(L - \bar{\Delta})}{L - \bar{\Delta} - \int_0^{L-\bar{\Delta}} ds \zeta(s)}, \quad (3.8)$$

where we have expanded for small  $\lambda$  and made use of  $\zeta(0) = 0$  far from the trap. For all practical purposes  $\lambda = -\gamma \zeta(L - \bar{\Delta})/L$ .

Since  $\lambda L \ll 1$  for most cases of experimental interest, the calculation of Section 2 applies in the region outside the trap (see Fig. 2) with the surface tension replaced by

$$\Sigma_0 \rightarrow \bar{\Sigma} = \Sigma_0 \zeta(L - \bar{\Delta}). \quad (3.9)$$

For a Gaussian shape  $\zeta(L - \bar{\Delta}) \lesssim 1$  [ $\zeta(L - \bar{\Delta}) \simeq 0.31$  in Fig. 3], so the modification to the naive boundary condition is rather minimal.

### 3.3. Trap Boundary Condition

To complete our discussion we estimate the stability against folding inside the trap. This determines the position  $\bar{\Delta}$  at which the boundary condition (3.2) applies, as well as a critical effective surface tension parameter (or laser intensity)  $\Sigma^*$  at which the system initiates flow. We imagine that the system has attained a steady state in the absence of buckling and flow, given by Eq. (3.5) with  $\lambda = 0$ :

$$a(z) = a_0 [1 - \gamma \zeta(z)]. \quad (3.10)$$

Here  $\gamma \zeta(z)$  is a measure of the compression.

Rather than calculating the stability of a patch with a non-uniform area per head  $a(z)$ , we calculate the stability against buckling of a patch with uniform  $a = \psi a_0$ , with  $\psi = 1 - \epsilon$ , and use the resulting critical strain  $\epsilon^*$  to determine  $\bar{\Delta}$  through

$$\gamma \zeta(L - \bar{\Delta}) \equiv \epsilon^*. \quad (3.11)$$

We consider perturbations  $R(z) = R_0(1 + u(z))$  which preserve the volume of the fluid. This constraint yields the condition  $\int [u(z)^2 + 2R_0 u(z)] = 0$  [15]. The free energy, which includes in-plane compression and bending, is <sup>(3)</sup>

$$2F = \int d^2r \left[ B \left( \frac{\psi a - a_0}{a_0} \right)^2 + \kappa H^2 \right], \quad (3.12)$$

where  $H$  is the mean curvature,  $a_0 = dzR_0$ , and  $a = \psi dzr$ . For the perturbation above [5],

<sup>(3)</sup>We do not include a term involving interaction with the laser, since we are interested in an instability at fixed particle number on the membrane.

$$d^2r = dz(R_0 + u(z))\sqrt{1 + u'(z)^2} \quad (3.13)$$

$$H = \frac{(1 + u'(z)^2)^{-1/2}}{R_0 + u(z)} - \frac{u''(z)}{(1 + u'(z)^2)^{3/2}}, \quad (3.14)$$

where  $u'(z) = du/dz$ .

To quadratic order in  $u(z) = \sum_q \hat{u}(q)e^{iqz}$  the energy per unit area  $A$  becomes [5]

$$\frac{2F}{A} = \sum_q \hat{u}(q)^2 \left[ \frac{3\kappa}{R_0} - 5BR_0\epsilon - \hat{q}^2 \left( 3BR_0\epsilon + \frac{\kappa}{R_0} \right) + 2\hat{q}^4 \frac{\kappa}{R_0} \right], \quad (3.15)$$

where  $\hat{q} = qR_0$ . The vanishing of the term in square brackets defines  $\epsilon^*$ , the minimum strain above which this energy is unstable to undulations. Combining this condition with our estimate for how  $\epsilon(z)$  varies away from the trap, Eq. (3.11), we find the following relation which determines  $\bar{\Delta}$ :

$$\sigma^* \equiv \frac{\Sigma^* R_0^2}{\kappa} = \frac{1}{\zeta(L - \bar{\Delta})} \frac{3 + 2\bar{q}^4 - \bar{q}^2}{5 + 3\bar{q}^2} \quad (3.16)$$

$$\equiv g(\bar{q}) \quad (3.17)$$

where  $\bar{q} \simeq \pi R_0 / \bar{\Delta}$ . For  $\sigma > \sigma^*$  the tubule should buckle inside the trap. Fig. 3 shows  $g(\bar{q})$  for the Gaussian laser spot.

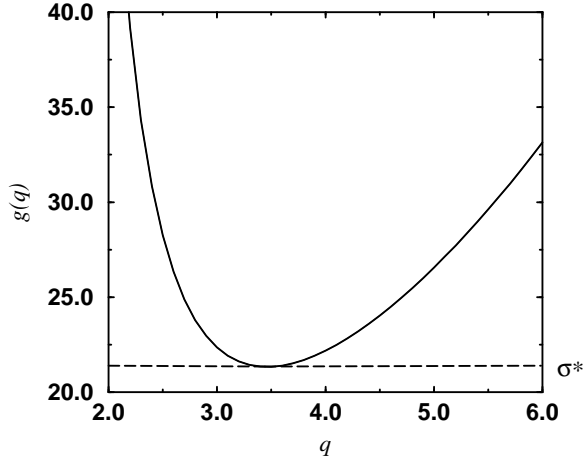


FIG. 3. Buckling criterion inside the laser trap for a laser spot size  $\Delta = 0.15 \mu\text{m}$  and tubule radius  $R_0 = 0.5 \mu\text{m}$ . Here, we find  $\sigma^* \simeq 21$ ,  $\bar{\Delta} \simeq 0.9R_0$ ,  $\zeta(L - \bar{\Delta}) \simeq 0.31$ , and  $\bar{\Sigma} \simeq 0.97\Sigma_0$ .

Our criterion depends on the trap shape, but not the compression modulus  $B$ . This happens because, while the strain induced in packing lipid in the trap varies as  $1/B$ , the critical strain at which buckling occurs is also inversely proportional to  $B$ , and the  $B$  dependence cancels out. In fact, the same order of magnitude estimate emerges from a comparison of bending and effective surface tension. What we have gained, however, is a picture of the forces at play that induce the buckling.

While our estimate apparently fails to predict buckling for typical values, relaxing a few approximations we have made should change this picture. First, we have assumed uniform coverage at the lowest value of the actual nonuniform coverage in the quiescent trap. Second, we have assumed an axisymmetric deformation. This is obviously not the case if the laser spot size is smaller than the tubule diameter. In addition, the volume constraint must be handled differently. Removing these approximations should, in both cases, result in a smaller  $\Sigma^*$ . For example, in the limit of small trap sizes we can ignore curvature and ask about the stability of a flat interface against buckling, for which the criterion above becomes

$$\Sigma^* = \frac{\kappa \bar{q}^2}{\zeta(L - \bar{\Delta})}. \quad (3.18)$$

demanding that the characteristic buckling wavevector  $\bar{q}$  be roughly the inverse of the trap size  $\bar{\Delta}$  determines the critical trap size and intensity. This is essentially the same estimate given by Bar-Ziv, Frisch, and Moses in a somewhat different context [16].

## 4. DISPERSION RELATION AND FRONT PROPAGATION

### 4.1. Dispersion Relation

We have shown thus far that, under steady-state conditions before any macroscopic shape instability occurs, the proper boundary conditions imply a surface tension gradient along the tubule which supports lipid flow. We now turn to the effects of this gradient. Rather than repeating the analysis of GNPS [7] with a non-uniform surface tension, we note that the characteristic wavenumber at which the instability occurs is typically  $q^* R_0 \simeq 0.8$ . Since  $R_0 \ll L$ , we suspect that the assumption of a locally constant surface tension along the tubule is a good first step. This allows us to transcribe the results of Ref. [7].

The primary result of interest is the growth rate  $\omega(q)$  of an undulation  $u(q, t)$ , where  $q$  denotes a Fourier mode along the tubule. This frequency is defined through

$$\left( \frac{\partial}{\partial t} + iq\bar{v} \right) u(q, t) = \omega(q) u(q, t), \quad (4.1)$$

where the convective term arises because the lipids have an average velocity.

In the original instability calculation presented by Rayleigh [2], and as has been emphasized in Refs. [1,6,5,7], the structure of  $\omega(q)$  is as follows:

$$\omega(q) = \Phi(q) T(qR_0). \quad (4.2)$$

The function  $T(qR_0)$  is determined by the energetics of the problem and, in our case, is non-zero for  $\Sigma R_0^2 / \kappa$  greater than a critical value of order unity [7,5]. In the

Rayleigh case the instability occurs for  $\Sigma > 0$ . The function  $\Phi(q)$  is determined by the dynamics of the problem, and it is here that much of the interesting and surprising physics lies. Energetics tells us that the most unstable modes are at low  $q$ , where undulations are the least ‘violent’, while dynamic considerations severely penalize the growth of modes in the limit  $q \rightarrow 0$ .

Goldstein *et al.* [7] calculated  $\omega(q)$  for a uniform surface tension  $\bar{\Sigma}$ , including the effects of bending as well as friction between the two bilayer leaves. Changing the boundary conditions of their work to allow for flux from the reservoir adds a convective term to the dynamics, and, aside from our local approximation above, changes nothing else. A plot of  $\omega(q)$  is shown in Figure 4 for several values of the surface tension  $\sigma = \bar{\Sigma}R_0^2/\kappa$ , with values for the bilayer friction and bulk modulus taken as in GNPS.

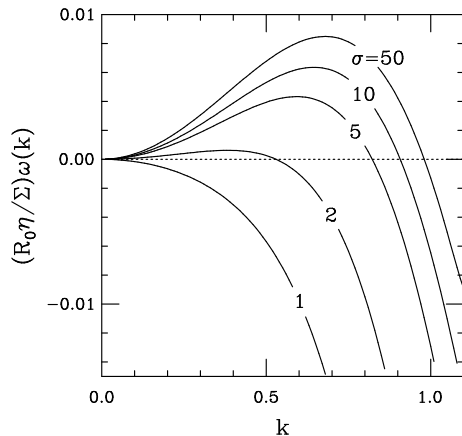


FIG. 4. Dispersion relation  $\omega(k)$ , with parameters as calculated by GNPS,  $\beta = 3.5$ ,  $\epsilon = 0.5$ . Reprinted from Ref. [7]. Alternatively, we may consider this as a plot of  $\omega(k, z)$  for  $\sigma = 50$  and  $z = L, L/5, L/10, L/25$ , and  $L/50$ . Here,  $k$  is in units of  $2\pi/R_0$ .

Since  $\sigma$  is  $z$ -dependent (Eq. 2.18), the growth rate  $\omega^*$  and wavenumber  $q^*$  of the fastest growing mode are  $z$ -dependent, and are greatest near the laser spot, as in Fig. 5. A single Fourier modulation has, locally, the following form: [7]

$$u(z, t) = u_0 e^{iq(z - \bar{v}t) + \omega(q, z)t}, \quad (4.3)$$

where  $\omega(q, z)$  is the function plotted as  $\omega(q)$  in Fig. 5 of Reference [7] and is reproduced here in Fig. 4. The  $z$ -dependence comes through the  $z$ -dependence of  $\sigma$ . Note that we rely *strongly* on the condition  $qL \gg 1$  [Note that in the experiments [1] with, say,  $L \simeq 200 \mu\text{m}$  and a diameter of  $1 \mu\text{m}$ , this condition is easily satisfied,  $qL \simeq 160$ .]

Given a dispersion relation which depends on position, there are several immediate naive predictions: The local wavenumber and apparent growth rate of the pat-

tern should decrease as the anchoring globules are approached, with the instability vanishing at a point close to the reservoir where the induced surface tension is not strong enough to overcome the barrier due to bending,  $\Sigma^* \simeq \kappa/R_0^2$ . Hence, in the experiments with  $\sigma \simeq 20$  [6], this occurs at  $1/20\text{th}$  of the distance from the anchoring globule to the laser trap. At points closer to the globule any undulation is a decaying remnant of the pattern developed closer to the trap.

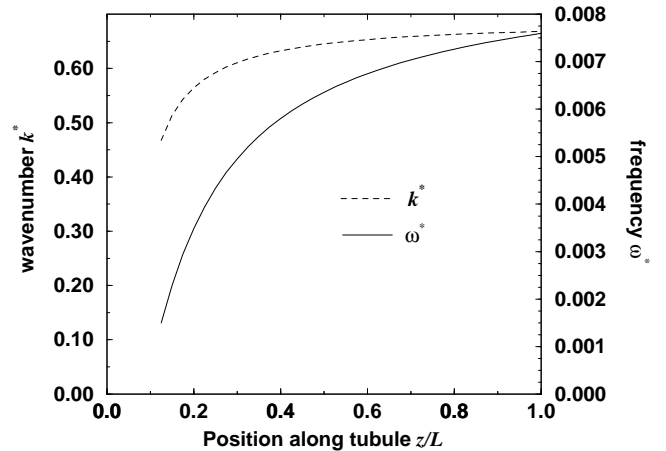


FIG. 5. Frequency  $\omega^*$  and dimensionless wavenumber  $k^*$  of fastest growing mode as a function of position along the tubule, obtained from Fig. 4 by taking  $\sigma(z = L) = 20$ .

## 4.2. Front Propagation

We now confront the issues of front propagation and wavelength selection. GNPS argued that the Marginal Stability Criterion hypothesis provides a reasonable estimate for both the propagation speed  $v_f$  and the selected wavenumber  $k^*$  [7]. A naive extension of this calculation, again assuming a local dispersion relation, predicts a spatially varying front speed and selected wavenumber. However, this prediction and the qualitative picture relies on two assumptions: (1) the existence of a propagating front, and (2) the absence of noise—i.e., that the propagation occurs into a uniform, unstable medium with no thermal fluctuations. The latter assumption is obviously not correct in detail, as thermal fluctuations, including modes of wavelengths comparable to the most unstable modes, are apparent in the experiments prior to the onset of the instability. Here we discuss these issues in the context of a spatially varying control parameter. Because a full treatment of the problem does not yet exist in the literature and is beyond the scope of this paper, we limit ourselves in this work to some numerical experiments and suggestions which, we hope, will stimulate further research on both this specific problem and the general aspects of front propagation into spatially-varying media in the presence of noise. For the rest of

this paper we refer to ‘noise’ as a set of random initial conditions which obey a Boltzmann distribution, and do not consider temporally fluctuating noise.

Kramer *et al.* [10], followed by others [17–19], showed that, in the presence of a ‘ramped’ control parameter that becomes subcritical at some point, as happens near the reservoir, the uniquely-selected wavenumber need not correspond to that determined by the MSC. This effect is expected to take precedence over the MSC-determined wavenumber at times after which non-linearities become important and the ‘phase’ of the pattern has time to diffuse of order the system size. However, we are concerned with the more fundamental issue of the *existence* of a propagating front.

In the presence of ‘noise’ which, in the present experiment, corresponds to existing thermal fluctuations around the reference smooth cylindrical state, a propagating front can be expected to exist for times less than the characteristic growth times of existing fluctuations in the vicinity of the most unstable mode. Hence, given a quench into an unstable ‘ramped’ state with an initial perturbation near the laser spot, propagation away from the perturbation occurs for an initial period of time, followed by rapid growth all along the cylinder as the initial conditions (‘noise’ of unstable wavelengths) are amplified to visible length scales. An initial perturbation near the laser spot is natural because, in practice, the laser spot diameter is smaller than the tubule diameter and a ‘pinching’ effect results whereby surfactant flows around the circumference of the tubule (as well as along the cylinder diameter) to fill the trap.

The effect of a ‘ramp’ in the control parameter should be most dramatic after the noise overwhelms the front propagation: for a flat control parameter (no ramp) the noise grows randomly everywhere, and the ‘front’ should break down when the noise has grown to visible amplitudes. However, for a steep enough ramp the non-uniform amplification of the noise could resemble front propagation.

To check these conjectures we have employed a simple caricature of the tubule dynamics, specified by

$$\left(\frac{\partial}{\partial t} + \bar{v}\partial_x\right)u(x, t) = [a(x)2k_0^2\partial_x^2 + \partial_x^4]u(x, t) - gu(x, t)^3, \quad (4.4)$$

where  $a(x)$  is a spatially varying control parameter chosen to mimic the dispersion relation and position dependencies in Figs. 4 and 5. A choice which gives reasonable qualitative agreement is

$$a(x) = \frac{|x - x_0|^{\alpha+1}}{(x - x_0)}, \quad (4.5)$$

where  $x_0$  is the point at which the system is absolutely unstable. We emphasize that this is a toy model whose details do not correspond to the Bar-Ziv *et al.* experiments, but which we believe contains the essential

physics of front propagation into an unstable inhomogeneous medium, as occurs in these experiments. For Fig. 5,  $x_0 \sim 0.05L$  and  $\alpha = 1/8$  are reasonable. Fig. 6 shows the local dispersion relation  $\omega^*(x)$  for various  $\alpha$ .

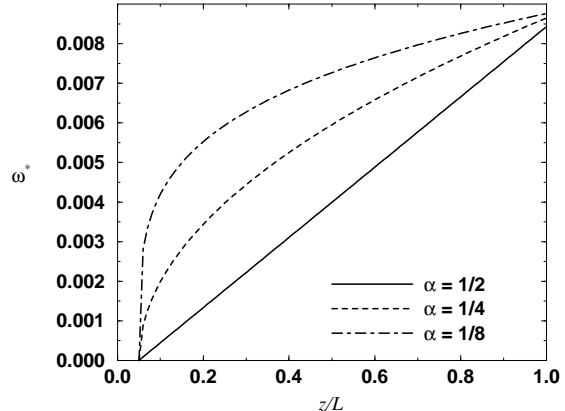


FIG. 6. Local dispersion relation  $\omega^*$  for trial form, Eq. (4.5), for  $\alpha = 1/2, 1/4, 1/8$ . The trap is at  $z/L = 1$ .

We have chosen the simplest possible non-linearity to stabilize the system. One may choose a more physical non-linearity such as the driving force arising from terms of higher than quadratic order in the mean curvature [7], but our purpose here is primarily to illustrate some qualitative behavior of a front propagating into a noisy, non-uniform media.

Figs. 7 and 8 show snapshots in the evolution of the system, given by Eq. (4.4), for an initial perturbation at the trap of 1% of the final amplitude (as determined by the non-linear term  $g$ ) and an initial condition (or ‘noise’) which is taken to be a superposition of 300 harmonics weighted with a Boltzmann weight corresponding to a non-zero surface tension (*i.e.* with an energy proportional to  $q^2$ ). We have chosen a system size of 150 wavelengths, and arbitrarily chosen the vertical scale to fill the figures.

The general features are as described above: a front ‘propagates’ for an initial time from the initial perturbation, after which the ‘noise’ takes over and a very irregular growth quickly overtakes the system.

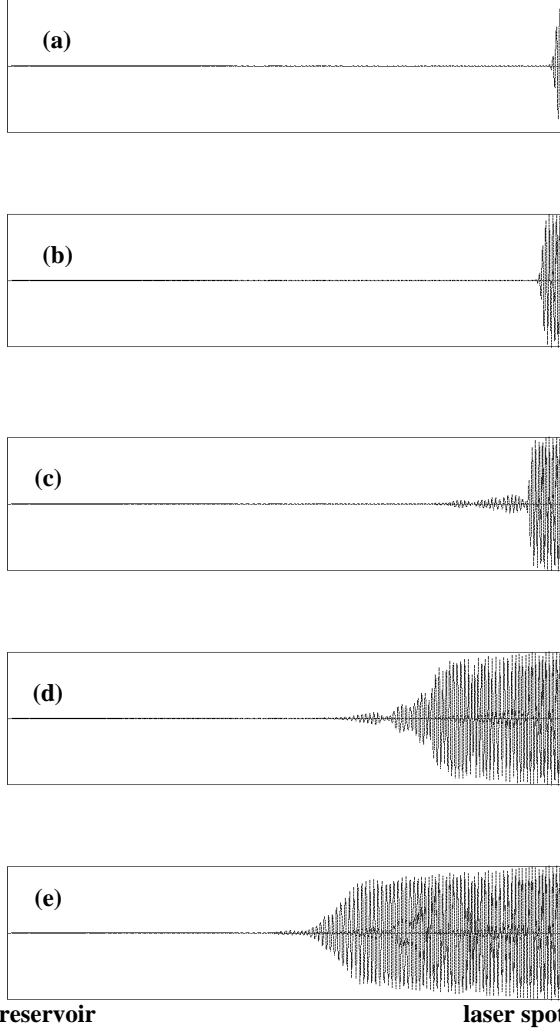


FIG. 7. Consecutive snapshots of  $u(x, t)$  as determined by Eq. (4.4). The conditions are: convection  $\bar{v} = 0$ ; initial perturbation at the laser spot  $u(L, t = 0) = 10^{-1}u(L, \infty)$ ; ramp parameter  $\alpha = 1/2$ ; initial mean noise amplitude a fraction  $10^{-6}$  of the final amplitude. Time intervals are every 80 time steps. The vertical scale is chosen to fit the amplitude of the undulation, and as such is a different scale than the horizontal scale. All snapshots have the same vertical scale. (a) and (b) show a propagating front; (c) and (d) show the acceleration due to amplification of the noise, and (e) shows a return to apparent propagation.

The steeper ramp ( $\alpha = 1/2$ , Fig. 7) has a better defined growth in the ‘noise’ regime, and could almost be called a ‘front’. In contrast, the growth into the shallow ramp ( $\alpha = 1/8$ , Fig. 8) is more ragged and it would be charitable to call this a front. The shallower ramp has a very slightly faster propagation speed in the initial regime, and an obviously faster ‘propagation’ speed in the noise-dominated regime. Both of these behaviors may be traced to the faster overall growth rate for a shallower ramp (where a larger fraction of the tubule is more unstable).

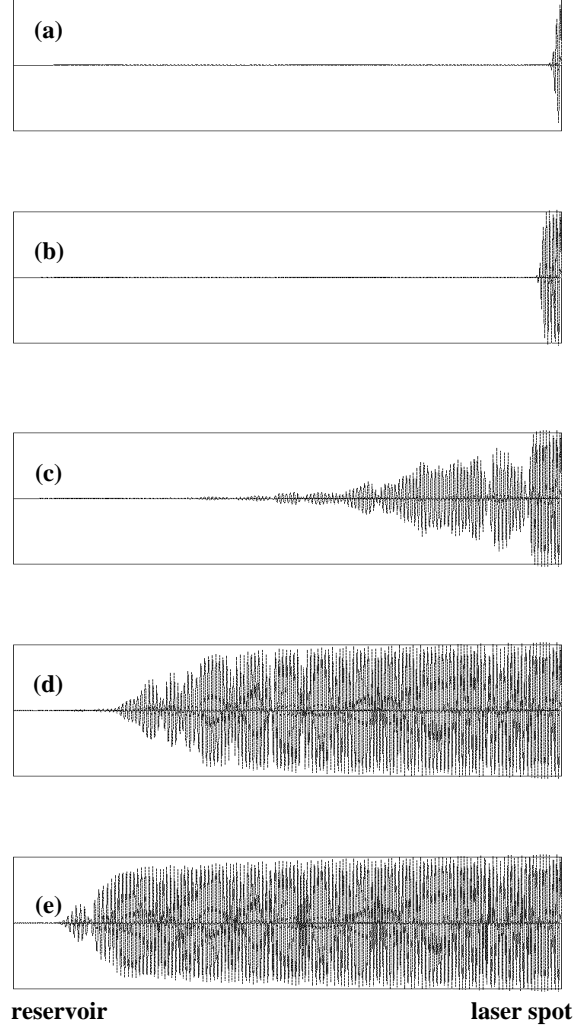


FIG. 8. Same parameters and time steps as in Fig. 7, except with ramp parameter  $\alpha = 1/8$ .

Fig. 9 shows the results of fixing the ramp and varying the noise amplitude. For a noisier system the effective propagation speed in the noise-dominated regime is faster, and the breakdown of the simple propagating regime occurs earlier. The propagation velocity before the noise takes over is independent of the noise amplitude. The delay before noise-dominance increases logarithmically with increasing noise amplitude, consistent with the simple argument that the propagating solution exists until the noise has grown to a given amplitude, since this initial growth is exponential.

To summarize, we have performed exploratory numerical calculations to investigate some of the consequences of a ramped control parameter, with an initial localized perturbation and initial global ‘noise’ for an initial condition, finding:

1. At early times a front propagates away from the localized perturbation. We find a dimensionless front

velocity of  $v\omega(k_0)/k_0 = 3.3$ , while the Marginal Stability Criteria [9] predict 4.6. A similar agreement was found in the simulations of GNPS [7].

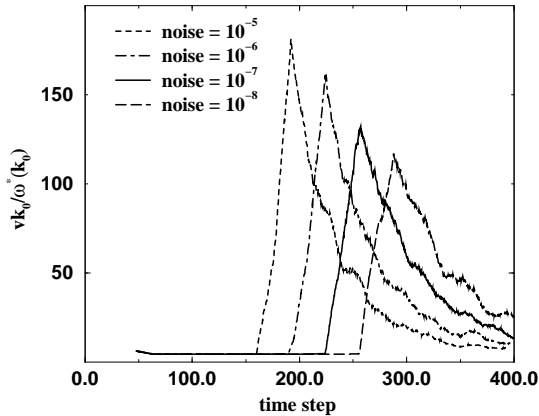


FIG. 9. Front velocity vs. time, averaged over 100 realizations of initial noise with weights described in the text. The velocity was measured by tracking the leading edge of the envelope of wavelets, and is plotted in units of the characteristic velocity  $\omega(k_0)/k_0$ , where  $\omega(k) = 2k_0^2 k^2 - k^4$  is the dispersion relation for Eq. (4.4) for  $a(x) = 1$ . Ramp parameter  $\alpha = 1/8$ . The noise is given as a fraction of the final amplitude.

2. In this first regime the propagation velocity is independent of noise amplitude.
3. After a time, which may be taken to be the time required for the ‘noise’ to grow to an observable amplitude, the unstable pattern rapidly develops everywhere on the tubule.
4. The speed and qualitative character of this growth depend on the noise and ramp characteristics. The growth is faster for a shallower ramp and/or stronger noise, and looks reminiscent of a front for a steeper ramp; and in all cases is much faster than the simple front propagation from the initial localized perturbation at the laser trap.

We have also performed calculations with no initial localized perturbation but, as this is probably not physically relevant, we do not report the results here. This initial study raises several questions which we feel are worth pursuing. In cases where the noise is weak enough and an apparent front exists, can this be understood quantitatively in terms of the gradient in the control parameter, and how does this relate to previous investigations of ‘ramped’ control parameters [10,17–19]? Can a ramp stabilize an advancing front?

## 5. CONCLUSION

## 5.1. Physical Picture

We have given the following picture of the action of lipid tubules upon the application of laser tweezers. In the absence of buckling, the laser induces a local compression of lipid molecules in the laser spot. This takes place in a time of order  $\tau_{ss} \sim 10^{-5}$ s. A sufficiently large laser intensity induces a local buckling of the membrane in the trap, which initiates flow down the tubule from the reservoir. We do not have an estimate of the delay time for the instability in the trap. In the absence of undulations *outside* the trap, this flow would build up to a steady-state value  $\bar{v} \sim 1 \mu\text{m s}^{-1}$  in a time order  $\tau_{ss}$ . The physics of this flow is a balance between drag against the bulk fluid and a force due to the gradient imposed by the chemical potential drop between the reservoir and the trap.

Given the steady-state tension profile within the membrane and the reasonable assumption that the gradient occurs over a length ( $L$ ) much larger than the critical wavelength ( $\sim R_0$ ), the analysis of GNPS [7] leads to a Rayleigh-like instability to undulations. This instability initiates near the laser spot where the chemical potential (or surface tension) is lowest, and propagates away from the spot to a point along the tubule at which the local surface tension falls below the critical tension  $\Sigma_{cr} = \kappa/R_0^2$  which characterizes the instability. Typical growth frequencies are  $\omega \sim 25 \text{ s}^{-1}$  [7], which corresponds to times  $\tau_\omega \sim 10^{-1}$ s. We note that the experiments find a significant time delay of order seconds before the instability, [20], a still-unexplained observation.

The estimate above for  $\tau_{ss}$  assumes a bare  $2D$  compression modulus  $B$ , while GNPS (see [13]) pointed out that  $B$  undergoes significant softening at the lengthscale of the tubule, due to the thermal fluctuations at low surface tension, and estimated a decrease of up to three orders of magnitude. This, correspondingly, would increase the value of  $\tau_{ss}$  to  $10^{-2}$ s, so that an accurate quantitative calculation must include the dynamics of the increase in surface tension. This leads to, effectively, a smaller applied tension  $\sigma$  and hence a slower propagation speed. This spirit was followed in the approach of Granek and Olami [5].

Our interpretation assumes that the trap accommodates material by folding, or some other means. Our analysis suggests that the proper boundary condition should be a fixed surface tension  $\bar{\Sigma} < \Sigma_0$  at the laser spot, where the laser shape determines  $\bar{\Sigma}$  through Eq. (3.9) and  $\bar{\Delta}$  through Eqs.(3.11,3.16).

This reservoir picture suggests that, upon turning off the laser, the system can revert to the original tubule by unfolding or, if severe topological changes have occurred (by, for example, budding in the laser spot or the creation of metastable ‘pearls’ as seen in the experiments), attain some other long-lived metastable state.

## 5.2. Discussion

In this work we have made several assumptions. The assumption that we can treat the anchoring globules as reservoirs presupposes that any damping processes regarding the transfer of lipid to and from the globules is negligible relative to other dynamical processes. We expect this to arise from the same source as the two-dimensional surface viscosity, which we have argued in Section 2.2 to be negligible. We have given a simplified picture of the scenario of trap buckling, where we take a single characteristic buckling wavevector, and treat the trap as uniform. This ‘single-mode’ approximation may be naive, and preliminary calculations suggest that the system is in fact less stable than this simple analysis would suggest [21]. There are also several other possible modes of instability which we have only mentioned but which could certainly play a role. We have also specified a boundary condition at the trap whereby the lipid relaxes to its preferred area per head group, which seems reasonable but is not otherwise justified. Finally, we have made a local approximation for the variation of the surface tension so that we may use the results of GNPS. This applies for sufficiently long tubules,  $L/R_0 \gg 1$ .

Front propagation and the detailed effects of propagating into a spatially-varying medium have only been touched upon in our numerical treatment. This study still leaves much to be resolved; one important question is how to accurately treat the non-linear regime. This has been treated in different ways by Olami and Granek [5] who considered the non-linear effect of removing surfactant from the membrane in the *absence* of a gradient, and by Goldstein *et al.* [7], who added the correct non-linear terms in the bending energy to examine the propagation of the pearls.

The primary new ingredients in our theory are (1) our treatment of the anchoring lipid globules as reservoirs and (2) our exploratory treatment of the role of pre-existing thermal fluctuations (noise) in determining the ‘front-like’ characteristics of the instability. Both Nelson and co-workers [6,7] and Olami and Granek [5] ‘turn off’ the reservoir. In the latter case material is drawn out of the existing thermal fluctuations, while Nelson and co-workers attribute the area change primarily to the shape instability itself. Olami and Granek impose a constant flux boundary condition at the trap, while Nelson and co-workers impose a fixed chemical potential  $-\bar{\Sigma}$  at the trap which, fairly rapidly, reduces the chemical potential everywhere to  $-\bar{\Sigma}$ . Our picture essentially gives the same boundary condition at the trap, but the treatment of the globule as a reservoir changes the qualitative picture dramatically.

Our theory differs from previous theories in several respects, and there are many consequences which may be checked experimentally. Obviously, we expect flow when an instability develops. This could be visualized by, for example, fluorescence spectroscopy with a very dilute

fraction of labelled lipids. The inhomogeneous surface tension implies that the local dispersion relation is also spatially-dependent, as in Fig 5, which implies that the velocity of front propagation  $v_f$  (which is proportional to  $\omega^*$  [7]) and characteristic wavenumbers should decrease farther away from the laser spot. Note that the characteristic wavelength changes very gradually compared to the speed of propagation, and as such would be more difficult to detect. It would also be interesting to see, experimentally, whether fluctuations are actually strong enough to destroy the front-like character, or whether two characteristic regimes exist in the experiments, as indicated in Fig. 9. Finally, we mention that the opportunity of using laser pulses to control flow within lipid and other systems presents amusing possibilities and applications.

## ACKNOWLEDGMENTS

It is a pleasure to thank E. Moses, R. Granek, P. Nelson, T. Powers, C.-M. Chen, S. Milner, and W. van Saarloos for helpful conversations and correspondence. This work was supported in part by NSF Grant No. DMR 92-57544 and by The Donors of the Petroleum Research Fund, administered by the American Chemical Society.

- 
- [1] R. Bar-Ziv and E. Moses, *Instability and “pearling” states produced in tubular membranes by competition of curvature and tension*, Phys. Rev. Lett. **73** (1994) 1392.
  - [2] Lord Rayleigh, *On the instability of jets*, Proc. Lond. Math. Soc. **10** (1879) 4.
  - [3] Lord Rayleigh, *On the instability of a cylinder of viscous liquid under capillary force*, Phil. Mag. **34** (1892) 145.
  - [4] S. Tomotika, *On the instability of a cylindrical thread of a viscous liquid surrounded by another viscous fluid*, Proc. Roy. Soc. Lond. **A150** (1932) 322.
  - [5] R. Granek and Z. Olami, *Dynamics of Rayleigh-like instability induced by laser tweezers in tubular vesicles of self-assembled membranes*, J. Phys. II (France) **5** (1995) 1349.
  - [6] P. Nelson, T. Powers, and U. Seifert, *Dynamical theory of the pearling instability in cylindrical vesicles*, Phys. Rev. Lett. **74** (1995) 3384.
  - [7] R. E. Goldstein, P. Nelson, T. Powers, and U. Seifert, *Front propagation in the pearling instability of tubular vesicles*, J. Phys. II (France) **6** (1996) 767.
  - [8] J. H. Schulman and J. B. Montagne, *Formation of microemulsions by amino alkyl alcohols*, Ann. N.Y. Acad. Sci. **92** (1961) 366.
  - [9] W. van Saarloos, *Front propagation into unstable states*, Phys. Rev. **A37** (1988) 211.
  - [10] L. Kramer, E. Ben-Jacob, H. Brand, and M. C. Cross, *Wavelength selection in systems far from equilibrium*, Phys. Rev. Lett. **49** (1982) 1891.

- [11] L. D. Landau and E. M. Lifschitz, *Fluid Mechanics* (Pergamon, Oxford, 1959).
- [12] E. Evans and D. Needham, *Physical properties of surfactant bilayer membranes: thermal transitions; elasticity; rigidity; cohesion; and colloidal interactions*, J. Phys. Chem. **91** (1987) 4219.
- [13] W. Helfrich and R.-M. Servuss, *Undulations steric interaction and cohesion of fluid membranes*, Nuovo Cim. **3D** (1984) 137.
- [14] M. B. Schneider and W. W. Webb, *Measurement of sub-micron laser beam radii*, Appl. Opt. **20** (1981) 1382.
- [15] S. A. Safran, *Statistical Thermodynamics of Surfaces, Interfaces, and Membranes* (Addison-Wesley, Reading, MA, 1994).
- [16] R. Bar-Ziv, T. Frisch, and E. Moses, *Entropic expulsion in vesicles*, Phys. Rev. Lett. **75** (1995) 3481.
- [17] J. B. Buell and I. Catton, *Wavenumber selection in ramped Rayleigh-Bénard convection*, J. Fluid Mech. **171** (1986) 477.
- [18] L. Kramer and H. Riecke, *Wavelength selection in Rayleigh-Bénard convection*, Z. Phys. B - Cond. Matt. **59** (1985) 245.
- [19] H. Riecke and H.-G. Paap, *Perfect wave-number selection and drifting patterns in ramped Taylor vortex flow*, Phys. Rev. Lett. **59** (1987) 2570.
- [20] E. Moses, private communication.
- [21] P. D. Olmsted and F. C. MacKintosh, unpublished (1996).